Proceedings of IMechE-I: Journal of Systems and Control Engineering, 2004, **218**, (I6), pp. 451–463

Dynamic Modelling and Open loop Control of a 2 DOF Twin Rotor Multi-Input Multi-Output System

S. M. Ahmad[1], **A. J. Chipperfield**[2] **and M. O. Tokhi**[3]

[1] School of Engineering, The University of Manchester, Manchester, M13 9PL, UK

[2]School of Engineering Sciences, University of Southampton, UK

[3] Department of Automatic Control and Systems Engineering, The University of Sheffield, Mappin Street, Sheffield, S1 3JD, UK.

Abstract

A dynamic model for the characterisation of a two-degree-of-freedom (DOF) twin rotor multi-input multi-output system (TRMS) in hover is extracted using a black-box system identification technique. Its behaviour in certain aspects resembles that of a helicopter, with a significant cross-coupling between longitudinal and lateral directional motions. Hence, it is an interesting identification and control problem. The extracted model is employed for designing and implementing a feedforward/open-loop control. Open-loop control is often the preliminary step for development of more complex feedback control laws. Hence, this paper also investigates open-loop control strategies using shaped command inputs for resonance suppression in the TRMS. Digital low-pass and band-stop shaped inputs are used on the TRMS test-bed, based on the identified vibrational modes. A comparative performance study is carried out and the results presented. The low-pass filter is shown to exhibit better vibration reduction. When modal coupling exists, decoupled feedback controllers are incapable of eliminating vibration. In such cases, generating motion by shaped reference inputs is clearly advantageous.

Keywords: Discrete-time systems, helicopter, linear identification, twin rotor MIMO system, open-loop control, vibration suppression.

NOTATION

ARMAX	auto-regressive moving average with exogenous input model
a_i, b_i, c_i,	unknown parameters to be identified
DC	direct current
$e(t)$	zero mean white noise
f	frequency, Hz
F1 and F2	thrust generated by the rotors in the vertical and horizontal planes respectively
H(jω)	frequency response magnitude
L	tuning parameter of the elliptic filter
na, nb, nc	orders of the *A*, *B*, and *C* polynomials of the ARMAX model
m	filter order
R_n	a rational function
S_{xx} and S_{yy}	auto power-spectral densities of input and output signals respectively
S_{xy}	cross-spectral density between pair of input and output signals
TRMS	twin rotor multi-input multi-output system
u1(t)	input to the main rotor (V)
u2(t)	input to the tail rotor (V)
y1(t)	pitch angle (rad)
y2(t)	yaw angle (rad)
δ_1, δ_2	filter attenuation
ε	band edge value
$\gamma^2_{xy}(f)$	ordinary coherence function
ω	radian frequency
ω_C	filter cut-off frequency
ω_p	pass-band edge frequency
ω_s	stop-band edge frequency
λ	parameter controlling height of ripple in an elliptic filter

1 Introduction

The last decade has witnessed a phenomenal growth in numerous fields, including robotics, space structures and unconventional air vehicles. The significant features of these endeavours have included the introduction of innovative design, exotic structural materials and sophisticated control paradigms. This is a striking departure from the beaten classical systems engineering philosophy. The focus of this paper, however, is restricted to the challenges and problems associated with flexible dynamical systems. Flexible structures, an area of intense interest in robotics [**1**-**3**] and spacecraft with flexible appendages [**4**-**6**] research, are attractive mainly because of their lightweight and strength. In aerospace vehicles [**7**, **8**] too, flexible airframe is adopted due to its lightweight, thereby improving the thrust to weight ratio for a given power plant. Desirability of achieving fast speed of response has prompted its use in systems such as flexible aircraft [**8**] and missile [**9**]. This has inadvertently increased the modelling efforts significantly. Thus, such flexible vehicles/systems cannot be modelled by the rigid body assumption alone. For instance, Waszak and Schmidt [**10**] demonstrated the inadequacy of a rigid 6 degrees-of-freedom (DOF) description of the dynamics of a high-speed transport aircraft with a moderate level of structural flexibility. Consequently, the flight controller performance based on inaccurate system model is thus palpable. Therefore, the need to account for aeroelastic effects will make modelling very crucial for such vehicles.

The second important issue connected with a dynamical flexible plant is that of motion induced vibration. The residual motion (vibration) is induced in flexible structures primarily as a result of faster motion commands. The occurrence of any vibration after the commanded position has reached will require additional settling time before the new manoeuvre could be initiated. Therefore, in order to achieve fast system response to command input signals, it is imperative to reduce this vibration. This feature is desirable in fast manoeuvring systems, such as fighter aircraft. Various approaches have been proposed to reduce vibration in flexible systems. They can be broadly categorised as open-loop (feedforward), closed-loop (feedback) or combination of feedforward and feedback methods. Some prior work in vibration control is briefly reviewed.

Suk *et al* [5] suggested and implemented torque-shaping approaches based on finite Fourier series expansion on a flexible space structure testbed (FSST). Another approach based on trigonometric series expansion is the work of Meckl *et al* [**11**] and references there in. A version of the approach using a pulse sequence expansion was suggested by Singer *et al*. [**3**]. However, the simplest method to achieve the resonance suppression is via classical digital filters, such as Butterworth, elliptic and Chebyshev [**1**, **2**].

Feedback or closed-loop approach utilises measurements and estimates of the system states to reduce vibration. Doughtery *et al* [12] and Franklin *et al* [**13**] applied classical control to space structures, to control the vibration and attitude (orientation). Recently, Teague *et al* [**6**] developed, a novel method for active control of the attitude and vibration of a flexible space structure using global positioning system (GPS) as a sensor. Linear quadratic regulator (LQR) feedback was applied in this study.

However, a suitable strategy for controlling a system with resonant modes is to use a combination of feedback and feedforward. The role of feedforward compensator is to place zeros near the lightly damped open-loop system poles, thereby creating "*notches*" at the corresponding resonant frequencies. The feedback loop, on the other hand, has a reduced task of controlling the rigid-body movement alone. This combined approach is particularly widely employed in aircraft control design, see [**14**] and references therein.

The twin issue of modelling and control of a dynamical flexible system, manifested in an experimental test rig, representing a *complex* twin rotor mulit-input multi-output (MIMO) system (TRMS), (Fig. 1), is addressed in this paper. The TRMS in addition to the rigid

degrees of freedom possess elastic degrees of freedom, thereby compounding the modelling and control efforts. Further aspects of the TRMS are given in Sections 2 and 3.

This paper will first briefly report the modelling aspects of a 2 DOF TRMS, a detailed account can be found in the authors' earlier work [**15**]. The second part will then utilise the modelling knowledge accrued in the first part to develop open-loop control strategies to attenuate system vibration. A shorter version of this work was presented at *IECON 2000* [**16**]. This work is a natural progression of the authors' investigation of a 1 DOF modelling and control problem [**17**].

The paper presents a feedforward control technique, which is related to a number of approaches known as "input shaping control", discussed above. The goal of this input shaping control is to avoid excitation of the residual vibration at the end of the manoeuvre. The fundamental concept for this type of control is based on the well-established theory of digital filters. In these methodologies, a feedforward input signal is shaped so that it does not contain spectral components at the system's resonance eigenfrequencies. The approach requires that the natural resonance frequencies of the system be determined through suitable identification and modelling techniques. Investigation of a MIMO open-loop control is a prelude to a future study, of the development of more complex multivariable feedback control laws.

The paper is organised as follows: Sections 2 and 3 describe the underlying motivation and experimental rig set up respectively. Section 4 briefly discusses modelling and presents the corresponding experimental results. Section 5 delves in the TRMS vibration mode analysis and control. Section 6 discusses filter design and implementation and Section 7 concludes the paper.

2 Motivation

Although, the TRMS shown in Fig. 1 does not fly, it has a striking similarity with a helicopter, such as system nonlinearities and cross-coupled modes. The TRMS, therefore, can be perceived as an unconventional and complex "air vehicle" with a flexible main body. These system characteristics present formidable challenges in modelling, control design and analysis. The TRMS is a laboratory set-up designed for control experiments by Feedback Instruments Ltd [**18**]. The main differences between a helicopter and the TRMS are as follows:

1. In a single main rotor helicopter the pivot point is located at the main rotor head, whereas in case of the TRMS pivot point is at midway between the two rotors.
2. In a helicopter, lift is generated via *collective pitch control,* i.e. pitch angles of all the blades of the main rotor are changed by an identical amount at every point in azimuth, but at the constant rotor speed. However, in the case of the TRMS, pitch angles of all the blades are fixed and speed control of the main rotor is employed to achieve vertical control.
3. Similarly, yaw is controlled in a helicopter by changing, by the same amount, the pitch angle of all the blades of the tail rotor. In the TRMS, yawing is affected by varying the tail rotor speed.
4. There are no *cyclical controls* in the TRMS, *cyclic* is used for directional control in a helicopter.

However, like a helicopter there is a strong cross-coupling between the *collective (main rotor)* and the tail rotor.

Although the TRMS rig reference point is fixed, it still resembles a helicopter, by being highly nonlinear with strongly coupled modes. Such a plant is thus a good benchmark problem to test and explore modern identification and control methodologies. The experimental set-up simulates similar problems and challenges encountered in real systems. These include complex dynamics leading to both parametric and dynamic uncertainty, unmeasurable states, sensor and actuator noise, saturation and quantization, bandwidth limitations and delays.

The presence of flexible dynamics in the TRMS is an additional motivating factor for this research. There is an immense interest in design, development, modelling and control of flexible systems, due to its utility in a multitude of applications for example in aerospace and robotics.

3 Experimental set-up

The TRMS considered in this work is described in Fig. 1. This consists of a beam pivoted on its base in such a way that it can rotate freely both in its horizontal and vertical planes. There are rotors (the main and tail rotors), driven by DC motors, at both ends of the beam. A counterbalance arm with a weight at its end is fixed to the beam at the pivot. The state of the beam is described by four process variables: yaw and pitch angles measured by position sensors fitted at the pivot, and two corresponding angular velocities. Two additional state variables are the angular velocities of the rotors, measured by tachogenerators coupled with the driving DC motors.

In a typical helicopter, the aerodynamic force is controlled by changing the angle of attack of the blades. The laboratory set-up is constructed such that the angle of attack of its blades is fixed, and the aerodynamic force is controlled by varying the speed of the motors. Therefore, the control inputs are supply voltages of the DC motors. A change in the voltage value results in a change of the rotational speed of the propeller, which results in a change of the corresponding angle (in radians) of the beam [**18**]. The main rotor produces a lifting force allowing the beam to rise vertically (p*itch angle/movement*), while the tail rotor, smaller than the main rotor, is used to make the beam turn left or right (y*aw angle/ movement*).

Aerodynamic modelling of air vehicles is generally carried out with either employing wind tunnel or using flight test measurements. In the former approach, static and dynamic tests are carried out on a scale model of the actual aircraft to obtain important aerodynamic derivatives. Important force-velocity and moment-velocity derivatives are estimated utilising six component force and moment balance. In the latter approach, on the other hand, modelling is accomplished by flying the air vehicle and subjecting it to different test signals to excite the system modes. Since carrying out flight tests on a full scale vehicle is prohibitively expensive and difficult, wind tunnel or laboratory scale tests like the ones described here are far more attractive.

4 System modelling

The objective of the identification experiments is to estimate a linear time-invariant (LTI) model of the 2-DOF TRMS in hover (refer Fig. 1(b)) without any *prior* system knowledge pertaining to the exact mathematical model structure, i.e. black-box modelling.

It is intuitively assumed that the rigid-body resonance modes of the TRMS lie in a low frequency range of 0-1 Hz, while the main rotor dynamics are at significantly higher frequencies. The rig configuration is such that it permits open-loop system identification, unlike a helicopter which is open-loop unstable in hover mode. In Fig. 2, the input signals *u1*

and *u2* represent voltage inputs to the main rotor and tail rotor respectively. The outputs *y1* and *y2* represent *pitch* and *yaw* angles in radians respectively. Strong coupling exists between the two channels, and this may be accounted for by representing the dynamics of the TRMS by the multivariable transfer function model given in Fig. 2.

System identification is carried out using a pseudo random binary sequence (PRBS) signal of 2 Hz bandwidth. The duration of the test signal was 120 seconds and a sampling interval of 10 Hz was chosen by trial and error. The details of MIMO system identification of the TRMS can be found in the previous work of the authors [**15**]. In this study, however, results will be presented briefly.

Strong interaction was observed among channels *u1* → *y1*, *u1* → *y2* and *u2* → y2, but not between *u2* → *y1* during the experimentation. These couplings between various channels were confirmed by coherence spectra [**15**]. Since no correlation exists between *u2* → *y1*, this channel was not investigated for model fitting.

4.1 Coupling analysis for a 2 DOF TRMS

The two modes of operation of the TRMS i.e. rotation in the vertical plane (*pitch*) and rotation in the horizontal plane (*yaw*), exhibit strong modal coupling. This coupling directly influences the velocities of the TRMS in both planes. The cross coupling through the *u1* → *y2* channel exists in the frequency range of interest i.e. 0-1 Hz, and is evident from the coherence spectrum of Fig. 3. The coherence function $\gamma^2_{xy}(f)$ is given by

$$\gamma^2_{xy}(f) = \frac{\left|S_{xy}(f)\right|^2}{S_{xx}(f)S_{yy}(f)} \tag{1}$$

where S_{xx} and S_{yy} are the auto-spectral densities of the input and output signals respectively and S_{xy} is the cross-spectral density between the input and output signals. By definition, the coherence function lies between 0 and 1 for all frequencies *f*;

$$0 \leq \gamma^2_{xy}(f) \leq 1$$

If *x*(t) and *y*(t) are completely unrelated, the coherence function will be zero. Thus, coherence of one indicates (coupled) a linear relationship between the two signals. And if the coherence function is equal to zero, it implies that the two signals are completely unrelated.

The implication of this coupling is that if motion in one direction contains energy at frequencies corresponding to mode shapes in another direction, then that motion will produce vibration in the other direction and could lead to instability. Hence, accurate identification and subsequent processing of these modes is important from a systems engineering perspective.

4.2 Mode or structure determination

Theoretically, the TRMS will have an infinite number of resonance modes with associated frequencies. However, it is intuitively assumed that the main dynamics (modes) of the TRMS lie in the 0-1 Hz range. It is further assumed that the rotor dynamics are at significantly higher frequencies than the rigid body modes. Investigations are carried out, under these broad hypotheses, to characterize the behaviour of the TRMS.

The power spectral density plot of the pitch (*y1*) and the *yaw* (*y2*) responses, see Fig. 4,

to the PRBS input (*u1*) signal, indicates closely spaced modes between 0-1 Hz, as expected. The *pitch* channel (*u1* → *y1*) has a main resonant mode at 0.34 Hz, and the *yaw* (*u1* → *y2*) channel at around 0.1 Hz. Hence, a model order of 2 or 4 corresponding to dominant modes for each channel is thus anticipated.

Similarly, for the 2nd input *u2* and 2nd output *y2* a model order of 2 or 4 is expected corresponding to the mode at 0.1 Hz, and a rigid-body (i.e. resonance frequency is zero) *yaw mode*, see Fig. 5. The results of identification are summarised in Table 1.

4.3 Parametric modelling

From the authors' earlier work [**15**] Auto-regressive moving average with exogenous input (ARMAX) model structure was found best to characterise the system dynamics. The ARMAX model is represented as

$$\begin{aligned} &y(t)+a_1y(t-1)+.....+a_{n_a}y(t-n_a)=b_1u(t-1)+.....+b_{n_b}u(t-n_b)+\\ &e(t)+c_1e(t-1)+....+c_{n_c}e(t-n_c) \end{aligned} \tag{2}$$

where, a_i, b_i, c_i, are the parameters to be identified, and, $e(t)$ is a zero mean white noise. This structure takes into account both the true system and noise models.

Power spectral density plots of the plant and the model outputs are superimposed in Figs. 4 and 5. It is observed that the dominant modes of models and the plant coincide quite well, implying good model predicting capability of the important system dynamics. Thus, it is assumed that the identified models are fairly accurate and suitable for open and/or closed loop controller design.

5 The TRMS vibration mode analysis

In general, for flexible structures/aircraft the parameter, which has an influence on the flexible modes is the mass distribution, which may change the frequencies of the modes and the accuracy of the model. In the case of an aircraft, the speed and Mach number also have an influence on the modes of the system. This is relevant to the TRMS, which can be interpreted as a centrally supported cantilever beam with loads (rotors) at both ends. The non-uniform mass distribution due to the rotors and the rotor torque at normal operating conditions are the main causes of beam deflection. The deflection of the beam is due to the excitation of the *resonance modes* by an input signal that is rich in system's eigenfrequencies. The different deflection profiles of the beam, occurring at corresponding resonance frequencies, represent system's *normal mode shapes.* Thus, in theory, the beam will have an infinite number of such normal modes with associated mode shapes and frequencies.

In conventional resonance, a dynamic system is excited by a fluctuating input, the frequency of which is equal to the natural frequency of the dynamic system. The TRMS could oscillate and become unstable if its natural frequency of oscillation is close or within the frequency range of the disturbance/excitation due to the rotor. A system or a structure will oscillate, and could become unstable, due to the excitation of the *resonance modes* by an input signal or disturbance that is rich in system's eigenfrequencies. Hence, accurate identification and subsequent processing of these modes is important from a systems engineering perspective. In particular, this is important for designing control laws to ensure that structural component limits and fatigue loads are not exceeded for the full operating range of aircraft/TRMS manoeuvres. Moreover, this will be useful for minimising structural

damage via resonant modes suppression, reduction in pilot workload and passenger comfort in the case of an aircraft. Similar advantages will result for other systems with elastic modes.

5.1 Open loop control

The presence of elastic modes as evident from the results in section 3 and summarised in Table 1, are the primary cause of residual vibration in the TRMS. Various approaches have been proposed to reduce vibration in flexible systems. These broadly include feedforward, feedback or combination of feedforward and feedback methods. Feedback control paradigm for 1 DOF has been investigated and reported by the authors in their recent work [**21**].

In this study, however, open-loop control methods are considered for vibration control where the control input is developed by considering the physical and vibrational property of the flexible system. The goal of this research is to develop methods to reduce motion and uneven mass induced vibrations in the TRMS during operation. The assumption is that the motion and the rotor load are the main sources of system vibration. Thus, input profiles, which do not contain energy at system natural frequencies do not excite structural vibration and hence require no additional settling time. Digital filters are used for pre-processing the input to the plant, so that no energy is ever put into the system near its resonance. The advantage of employing shaped reference inputs when modal coupling exists, as is the case with the TRMS, would be evident from the results.

5.2 Digital filters for command shaping

In order to filter out the input energy at the system's natural frequencies two different mechanisms can be adopted. The first approach is to pass the command signal through a low-pass filter. This will attenuate input energy at all frequencies above the filter cut-off frequency. An important consideration is to achieve a steep roll-off rate at the cut-off frequency so that the input energy can be passed for frequencies close to the lowest natural frequency of the TRMS. Another approach that can be employed to attenuate input energy at plant natural frequencies is to use band-stop filters with centre frequencies at selected significant resonance modes of the TRMS.

Different types of filter, such as Butterworth, elliptic and Chebyshev can be used. In this study mainly Butterworth type is employed because of its simple design and in particular as its pass-band and stop-band are without ripples. The elliptic type filter is also employed as a band-stop filter in the latter part of this work, primarily because it has a short transition region from pass-band to stop-band.

The Butterworth filter is called the *maximally flat filter* because of lack of ripple in the passband. However, the Butterworth filter achieves its flatness at the expense of a relatively wide transition region. The Butterworth filter is defined by the squared magnitude transfer function [**19**]:

$$\left|\mathrm{H_B}(j\omega)\right|^2 = \frac{1}{1+\left[\dfrac{\omega}{\omega_\mathrm{C}}\right]^{2\mathrm{m}}} = \frac{1}{1+\varepsilon\left[\dfrac{\omega}{\omega_\mathrm{P}}\right]^{2\mathrm{m}}} \tag{3}$$

where, *m* is the order of the filter and ω_C, is the filter cut-off frequency, ω_p is the pass-band edge frequency and $(1+\varepsilon^2)^{-1}$ is the band edge value of $\left|\mathrm{H_B}(j\omega)\right|^2$. Thus from the above

equation the filter order needed to achieve attenuation δ_2 at a particular frequency is easily obtained as:

$$m = \frac{\log(1/\delta_2^2 - 1)}{2\log(\omega_s / \omega_p)} = \frac{\log(\delta_1 / \varepsilon)}{\log(\omega_s / \omega_p)} \tag{4}$$

where, by definition, $\delta_2 = (1+\delta_1^2)^{-0.5}$. Therefore, the Butterworth filter is completely described by the parameters δ_2, *m,* ε and the ratio ω_s / ω_p . This equation can be utilised with arbitrary δ_1, δ_2, ω_C, and ω_s to yield the desired filter order *m* from which filter design is easily obtained..

The elliptic filter has the shortest transition region from pass-band to stop-band of any filter with the same order and ripple heights. The elliptic design is optimum in this sense. Therefore, the elliptic filter is ideal for applications where ripples can be tolerated and short transition regions are demanded. The squared magnitude transfer function of the elliptic filter is given as:

$$\left|H_E(j\omega)\right|^2 = \frac{1}{1+\lambda^2\left[R_n\left(\frac{\omega}{\omega_c}, L\right)\right]^2} \tag{5}$$

where, the parameter λ controls the height of ripples and ω_C controls the frequency breakpoint. R_n is a rational function, the parameter L controls the width of the transition region, the ripple height in the stop-band, and interacts with ω_C to affect the breakpoint [**20**]. The design of elliptic filters is much more complex than Butterworth and Chebyshev types. This is because the designer must select the order of the filter, the cut-off frequency, and the parameter L. The design is further complicated because ω_C and L interact in determining the filter's breakpoint. For this reason, elliptic filters are designed via design tables, given in most standard textbooks [**22**].

The open-loop control experiments are conducted for a 2 DOF TRMS, allowing movement in both the horizontal and vertical planes. Note, that the significant modes of the TRMS identified in Section 3 that need attenuation are given in Table 1 for the 2 DOF plant. Analogous to modelling, the sampling interval of 10 Hz is used for 2 DOF control experiments. The TRMS operating point is the flat horizontal position of the beam.

6 Implementation and results

To study system performance initially an unshaped doublet input shown in Fig. 6 is used, to drive the main rotor (*u1*) and the corresponding system responses *y1* and *y2* are measured (see solid lines of Figs 7 and 8). The response overshoots and shows considerable residual vibration, with dominating modes at 0.1 Hz and 0.31 Hz. The procedure is then repeated, exciting the tail rotor (*u2*), using the same input, as above. The response *y2* is shown in Fig. 9 by solid lines. Even here the response overshoots, however with mild residual vibration. The dominant mode in this axis lies at 0.1 Hz. The main objective of this section is to suppress the system vibrations at the first few dominant resonance modes in both axes simultaneously. Two different types of strategies can be adopted to filter out the input energy at the natural

frequencies. The first approach is to pass the input through a low-pass filter. This will attenuate input energy at all frequencies above the cut-off frequency. An alternative approach is to remove energy at system's natural frequencies by employing narrow-band band-stop filters, with centre frequencies selected at dominant resonance modes of the system. In this work both these methods are investigated, employing low-pass Butterworth and band-stop elliptic filters. Finally, Table 2 summarises the results of the open-loop control experiments.

6.1 Low-pass shaped input

A low-pass Butterworth filter of order three with a cut-off frequency at 0.05 Hz was designed and employed for off-line processing the doublet input. The motive behind selecting the cut-off frequency at 0.05 Hz lies in the fact that the lowest vibrational mode of the system is found to be at 0.1 Hz. Hence, to attenuate resonance of the system the cut-off frequency must be selected lower than the lowest vibrational mode. The shaped doublet input is then injected in the main rotor (*u1*) of the TRMS and the *pitch* (*y1*) and *yaw* (*y2*) responses are measured. The low-pass Butterworth filtered doublet is shown in Fig. 6 and the corresponding *pitch* and *yaw* responses in Figs. 7 and 8. It is noted that the attenuation in the level of vibration at the first and second resonance modes of the *u1* → *y1* channel are 10.45 dB and 20.91 dB respectively, as shown in Fig. 7, with the shaped input in comparison to the unshaped doublet. An attenuation of 24.22 dB is achieved for the *u1* → *y2* channel, see Fig. 8.

For the *u2* → *y2* channel, a spectral attenuation of 10.63 dB is obtained using the shaped input as is evident from Fig. 9. Notice that the cut-off frequency of 0.05 Hz, which is very close to the rigid-body motion dynamics, results in substantial attenuation of the input to the rigid-body mode. This is reflected in the low magnitude responses as compared to the unshaped responses.

6.2 Band-stop shaped input

As before, a second order digital elliptic filter was used to study the TRMS performance with a band-stop shaped input. For effective suppression of the vibrations of the system, the centre frequency of the band-stop filter has to be exactly at the same frequency or as close as possible to the resonance frequency. From Table 1, it is observed that the main resonant mode lies at 0.1 Hz and 0.34 Hz for the *u1*→ *y1* channel and at 0.1 Hz for the *u1* → *y2* and u2 → *y2* channels. Thus, three filters with different stopband frequency ranges were investigated i) 0.25-0.4 Hz ii) 0.05-0.15 Hz and 0.25-0.4 Hz iii) 0.05-0.15 Hz. A band-stop shaped doublet input, shown in Fig. 10 by dotted and dashed lines, was used and the responses were measured.

It is observed from Fig. 11(b), that the dominating 0.34 Hz vibration mode has been reduced by almost 14 dB with the use of Filter 1. The time-history reveals reasonable damping and residual vibration disappearing quickly. Obviously this filter has no bearing on the *u1* → *y2* channel. The shaped input has not lost much of its profile, hence the response *y1* is fairly smooth. The intent in using this filter i.e. just suppressing 0.34 Hz mode, was to gauge the system performance and compare it with the performance of Filter 2.

Filter 2 is designed to suppress prominent resonant modes appearing in both the channels. Some observations are noted for this filter:

1. shaped input is badly distorted, hence good tracking of the command is unlikely

2. time-history of Figs. 11, 12, and 13 display good damping (i.e. no overshoot) and minimal residual vibrations
3. the response *y1* is not smooth, indicating inconsistent and attenuated kinetic energy supply to the system.
4. as in the case of a low-pass filter, a band-stop frequency very close to the rigid-body mode, results in significant deterioration of the output magnitude and shape.
5. it is noted that the spectral attenuation in the system vibration at the first (0.1 Hz) and second (0.34 Hz) mode are 20 dB and 13.98 dB respectively for the *u1* → *y1* channel (Fig. 11) and 36.25 dB for *u1* → *y2* channel (Fig. 12).

Filter 3, was employed for the *u2* → *y2* channel (Fig. 13), and resulted in vibration reduction of 18.59 dB. The results of the MIMO open-loop experiments are summarized in Table 2.

7 Conclusion

A 2 DOF TRMS model, whose dynamics resemble that of a helicopter, has been successfully identified. The extracted model has been employed for designing and implementing open-loop control.

A feedforward control technique, which is related to a number of approaches known as "input shaping control", has been investigated. In these methodologies an input signal is shaped so that it does not contain spectral components at system's resonance eigenfrequencies. The study revealed that better performance in attenuation of system vibration at the resonance modes is achieved with low pass filtered input, as compared to band-stop filter. This is due to indiscriminate spectral attenuation at frequencies above the cut-off frequency in the low-pass filtered input. However, this is at the expense of slightly longer move time as compared to band-stop filter.

Open-loop control presents several advantages, a) it reduces the settling time of the commanded manoeuvre, hence subsequent command signals can be processed quickly, thereby making the system response fast, b) vibrational modes are suppressed, therefore improving the stability characteristics of the system, and c) feedback controllers for MIMO systems are generally designed for each channel and are decoupled from the other channels. If modal coupling exists, they cannot eliminate vibration caused by the motion in the other channels. However, this type of vibration can be effectively suppressed by shaped reference inputs.

Open-loop control using digital filters forms an important preliminary part of closed loop control design, in particular for flexible systems like flexible aircraft/TRMS. This is a topic of future investigation.

Acknowledgements

S.M.Ahmad gratefully acknowledges the financial support of the University of Sheffield and the Department of Automatic Control and Systems Engineering. The authors would also like to thank Dr.H.A.Thompson, Manager, Rolls-Royce University Technology Centre in Control and Systems Engineering, the University of Sheffield, for many valuable comments on helicopter dynamics.

References

1 **Tokhi, M. O.,** and **Azad, A. K. M**. Active vibration suppression of flexible manipulator system open-loop control methods, *International Journal of Active Control,* 1995, **1**(1), pp 15-43.

2 **Poerwanto, H**. Dynamic simulation and control of flexible manipulators systems, Ph.D thesis, 1998, Department of Automatic Control and Systems Engineering, The University of Sheffield, UK.

3 **Singer, N. C.,** and **Seering, W. P.** Preshaping command inputs to reduce system vibration, ASME *Journal of Dynamics Systems, Measurement, and Control,* 1990, **112**(1), pp 76-81.

4 **Dimitry, G., and Vukovich, G**. Nonlinear input shaping control of flexible spacecraft reorientation maneuver, *Journal of Guidance, Control, and Dynamics,* 1998, **21**(2), pp.264-269.

5 **Suk, J., Kim, Y.** and **Bang H.** Experimental evaluation of the torque-shaping method for slew maneuver of flexible space structures, *Journal of Guidance, Control, and Dynamics,* 1998, **21**(6), pp.817-822.

6 **Teague, E. H., How, J. P.** and **Parkinson, B.W.** Control of flexible structures using GPS: methods and experimental results, *Journal of Guidance, Control, and Dynamics,* 1998, **21**(5), pp.673-683.

7 **Livet, T., Fath, D.** and **Magni, J.F.** Robust flight control design with respect to delays, control efficiencies and flexible modes, *Control Eng. Practice,* 1995, **3**(10), pp.1373-1384.

8 **Livet, T., Fath, D.** and **Kubica F.** Robust autopilot design for a highly flexible aircraft, IFAC'96, San Francisco, CA, USA. Preprints, 1996, Vol. P, pp 279-284.

9 **George, K. K.,** and **Bhat, M. S.** Two-degree-of-freedom H-∞ robust controller for a flexible missile, *Journal of Guidance, Control, and Dynamics,* 1998, **21**, 518-520.

10 **Waszak, M. R. and Schmidt, D. K.** Flight dynamics of aeroelastic vehicles. *Journal of Aircraft*, 1988, **25**, 263-271.

11 **Meckl, P.H.,** and **Seering, W. P.** Experimental evaluation of shaped inputs to reduce vibration of a Cartesian robot, *Trans. of the ASME Journal of Dynamic Systems, Measurement and Control,* 1990, **112**(6), pp. 159-165.

12 **Dougherty, H., Tompetrini, K., Levinthal, J.,** and **Nurre, G.** Space telescope pointing control system, *Journal of Guidance, Control, and Dynamics,* 1982, **5**(4), pp. 403-409.

13 **Franklin, G. F., Powell, J.D. and Emami-Naeini, A**. *Feedback control of dynamic systems,* 1998 (Addison-Wesley, Reading, Massachusetts).

14 **Blight, J. D., Dailey, R. L. and Gangsaas, D.** Practical control law design for aircraft using multivariable techniques. In M.B. Tischler (Ed) Advances in Aircraft Flight Control, 1996 (Taylor & Francis, London), pp 231-267.

15 **Ahmad, S. M., Chipperfield, A. J.** and **Tokhi, M. O.** Parametric modelling and dynamic characterization of a two-degree-of-freedom twin rotor multi-input multi-output system. *Proc. Instn Mech. Engrs, G: J. Aerospace Engng*, 2001, **215**(**G2**), 63-

78.

16 **Ahmad, S. M., Chipperfield, A. J.** and **Tokhi, M. O.** Dynamic modelling and control of a 2 dof twin rotor Multi-Input Multi-Output system, In Proc. IEEE Industrial Electronics, Control and Instrumentation Conference (IECON'2000*),* Nagoya, Japan, 22-28 Oct. pp 1451-1456.

17 **Ahmad, S. M., Chipperfield, A. J.** and **Tokhi, M. O.** Dynamic modelling and open loop control of a twin rotor MIMO system. *Proc. Instn Mech. Engrs, Part I: J. Systems and Control Engineering*, 2002, **216**(16), 477-496.

18 **Feedback Instruments Ltd.** *Twin rotor MIMO system*, Manual 33-007-0, 1996 (Feedback Instruments Ltd., Sussex, UK).

19 **Jackson, L. B.** *Digital filters and signal processing,* 1989 (Kluwer Academic Publishers, London).

20 **Williams, C. S.** *Designing digital filters*, 1986 (Prentice Hall, NJ).

21 **Ahmad, S. M., Chipperfield, A. J.** and **Tokhi, M. O.** Dynamic modelling and linear quadratic Gaussian control of a twin-rotor multi-input multi-output system," *Proc. IMechE Part I: Journal of Systems and Control Engineering*, 2003, **217**, pp. 203–227.

22 **Dwight, H. B.** *Tables and integrals and other mathematical data*, 1958 (3rd Ed., Macmillan, New York).

TABLES

DOF	**Channel**	**Identified system modes**
Two	*u1* → *y1*	0.1 Hz and 0.34 Hz
	u1 → *y2*	0.1 Hz
	u2 → *y2*	0.1 Hz
	u2→ *y1*	No cross coupling

Table 1. Identified natural frequencies.

		Filter-1 [0.25-0.4] Hz	**Filter-2 [0.01-0.15; 0.25-0.4] Hz**	**Filter-3 [0.05-0.15] Hz**	**Lowpass cut-off [0.05] Hz**
u1→ *y1*	0.1		20 dB		10.45 dB
	0.34	13.98 dB	13.98 dB		20.91 dB
u1→ *y2*	0.1		36.25 dB		24.22 dB
u2→ *y2*	0.1			18.59 dB	10.63 dB

Table 2. MIMO open-loop control**:** mode attenuation.

FIGURES

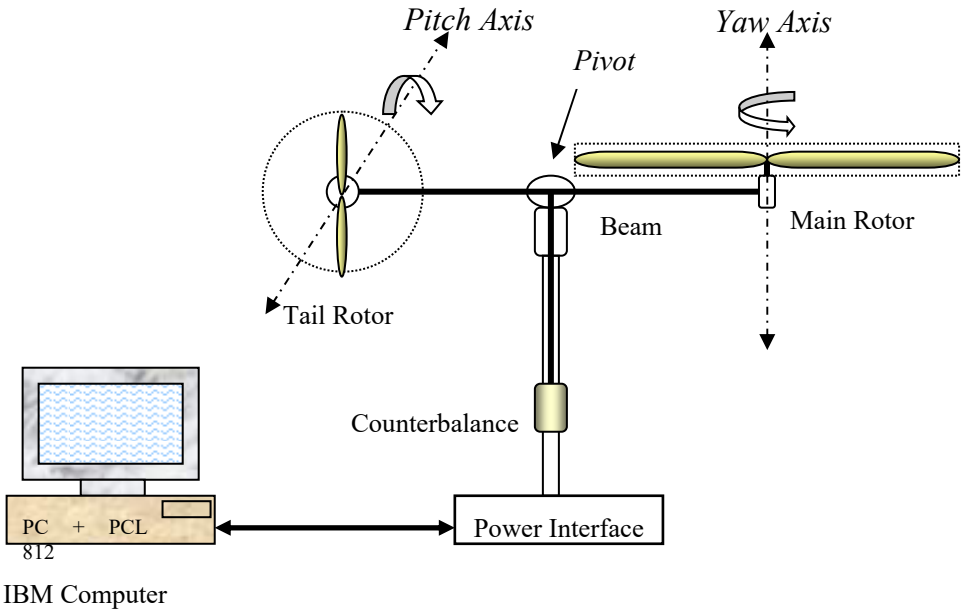

Fig. 1(a) The twin rotor MIMO system schematic diagram.

Fig. 1(b) The TRMS in "hover" mode.

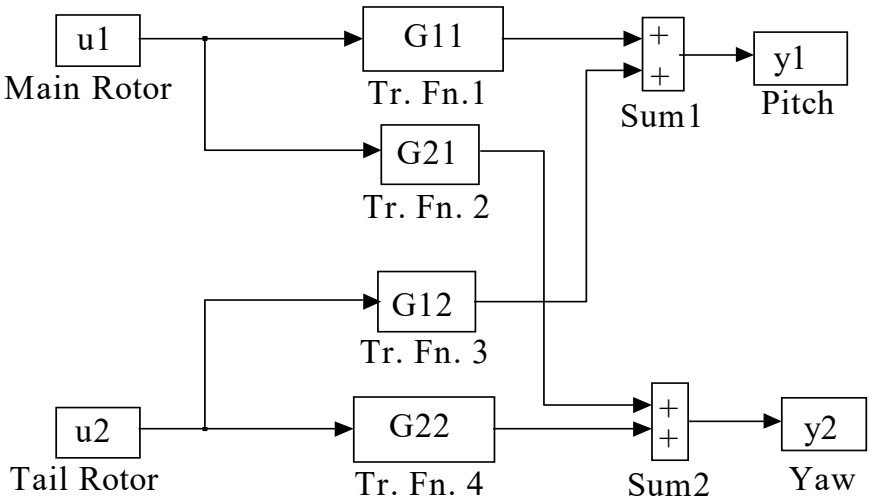

Fig. 2 MIMO transfer function model.

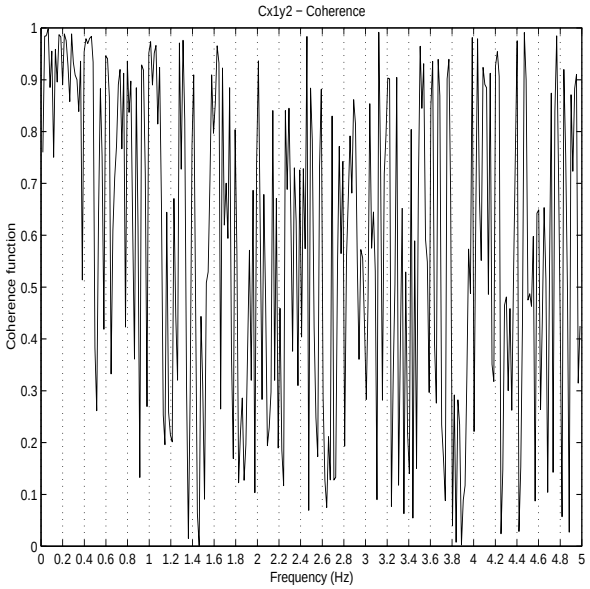

Fig. 3 Coherence spectrum, *u1* → *y2* channel.

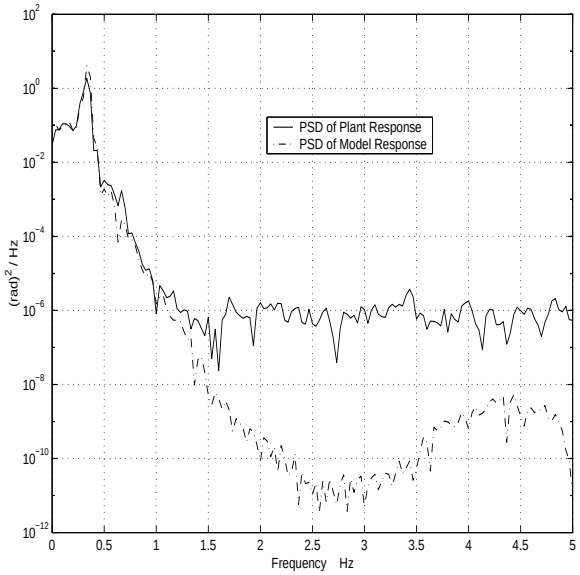

(a) Pitch response, *u1* → *y1*

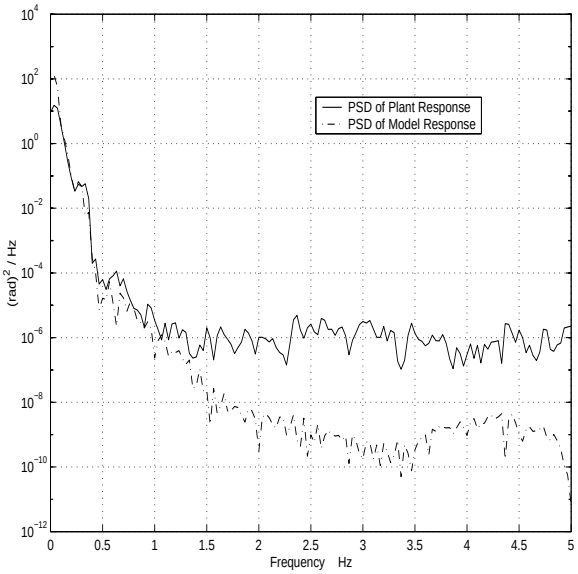

(b) Yaw response, *u1* → *y2*.

Fig. 4 Power spectral density.

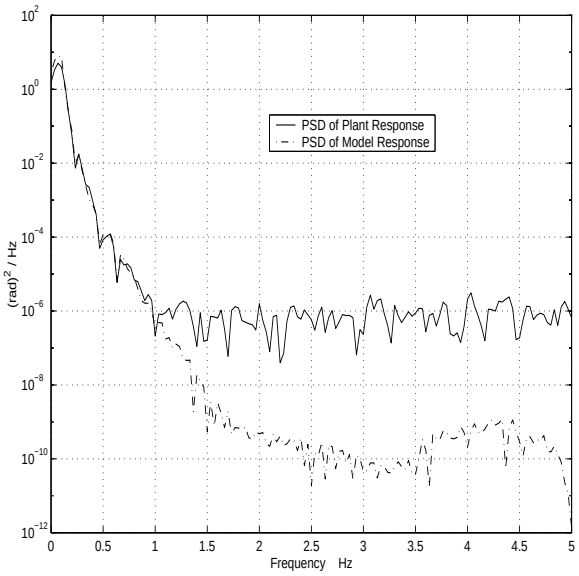

Yaw response, *u2* → *y2*.

Fig. 5 Power spectral density.

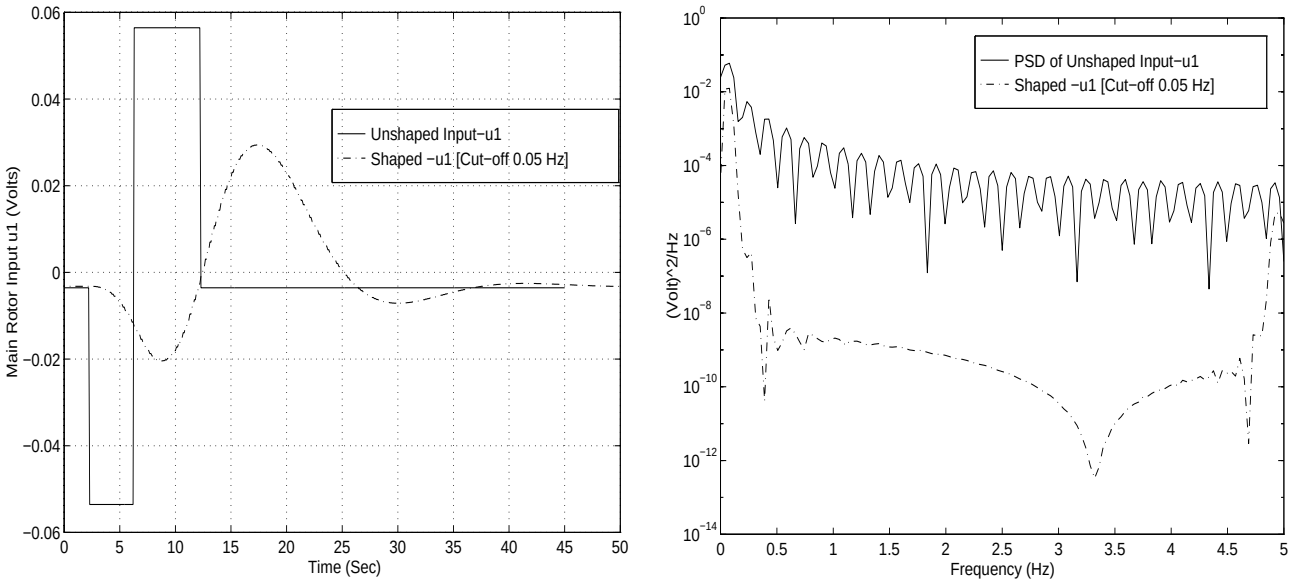

(a) Time domain. (b) Power spectral density.

Fig. 6 Doublet input using a low-pass filter.

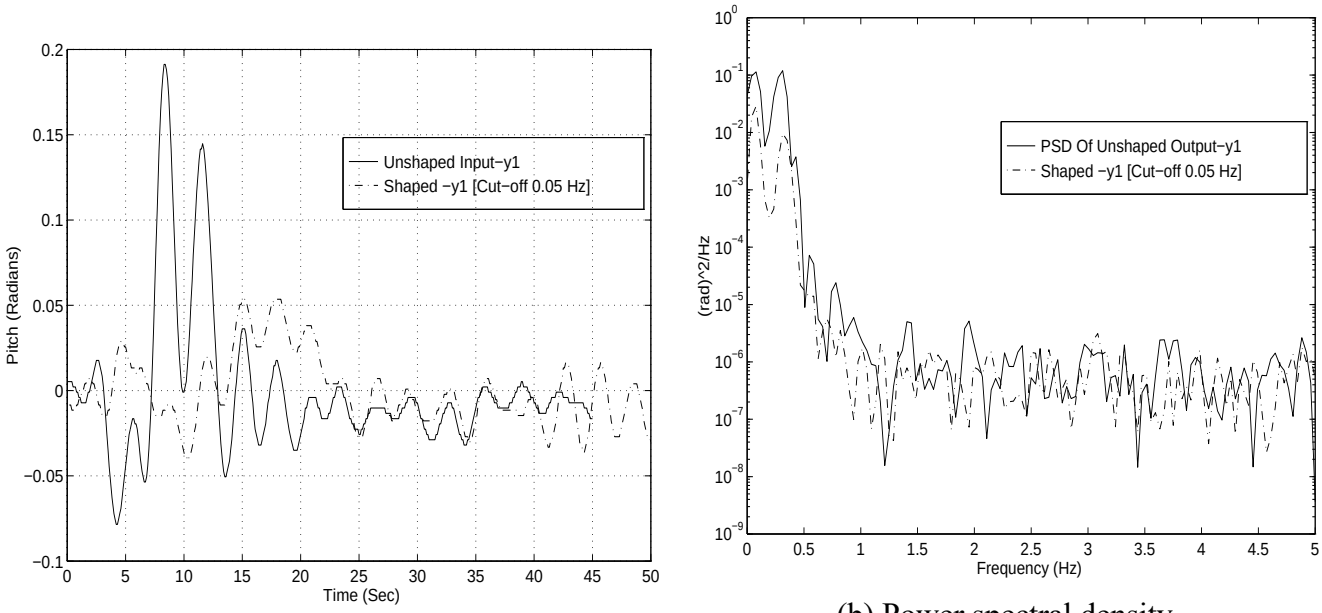

(a) Time domain. (b) Power spectral density.

Fig. 7 Pitch response to a low-pass filtered doublet input, *u1* → *y1*.

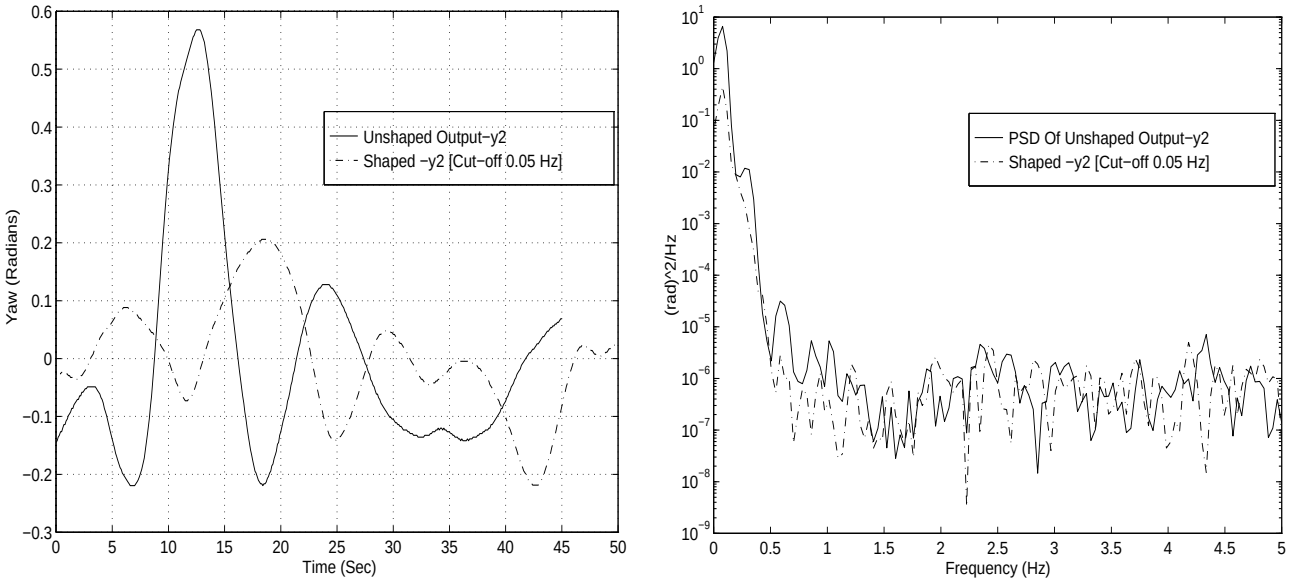

(a) Time domain. (b) Power spectral density.

Fig. 8 Yaw response to a low-pass filtered doublet input, *u1* → *y2*.

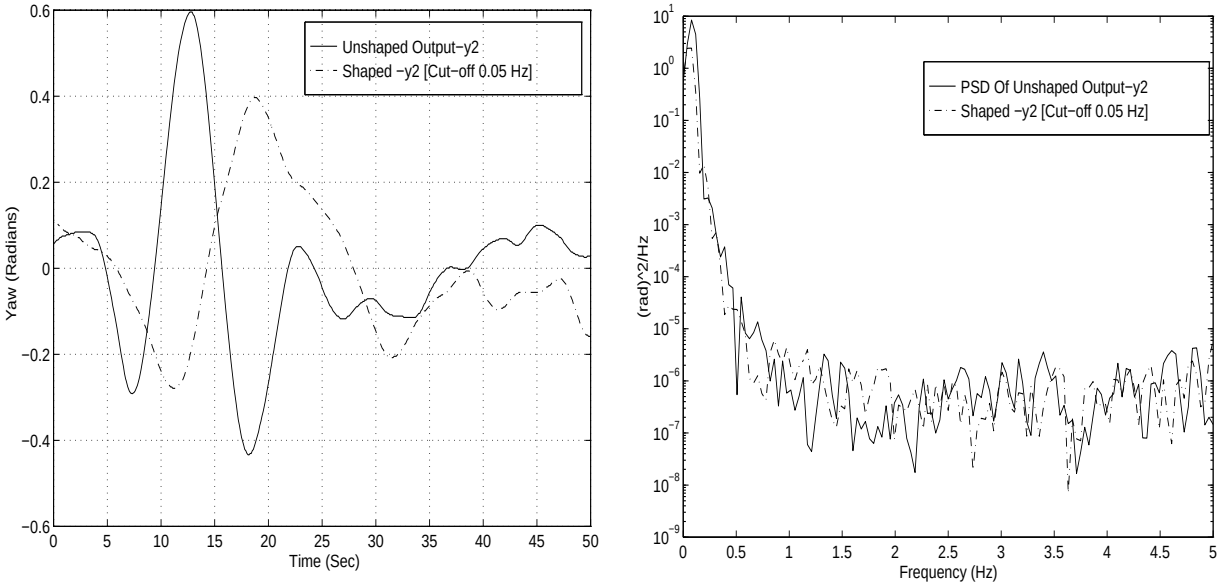

(a) Time domain. (b) Power spectral density.

Fig. 9 Yaw response to a low-pass filtered doublet input, *u2* → *y2.*

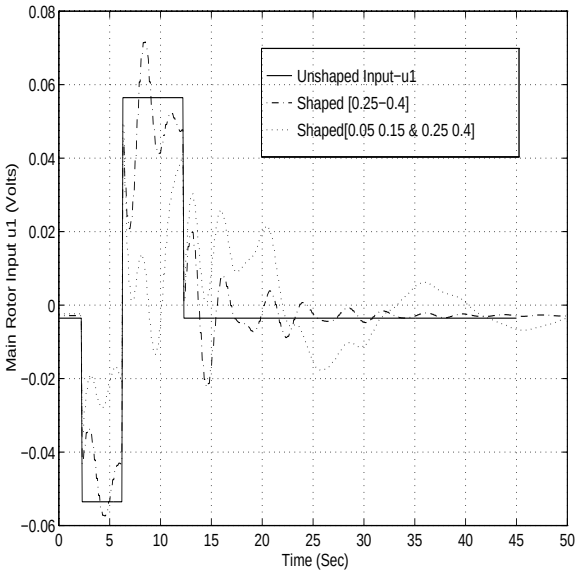

(a) Time domain.

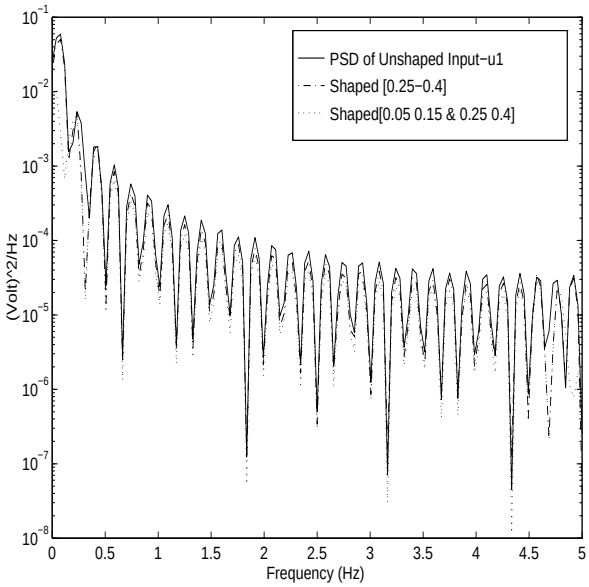

(b) Power spectral density.

Fig. 10 Doublet input using band-stop filter.

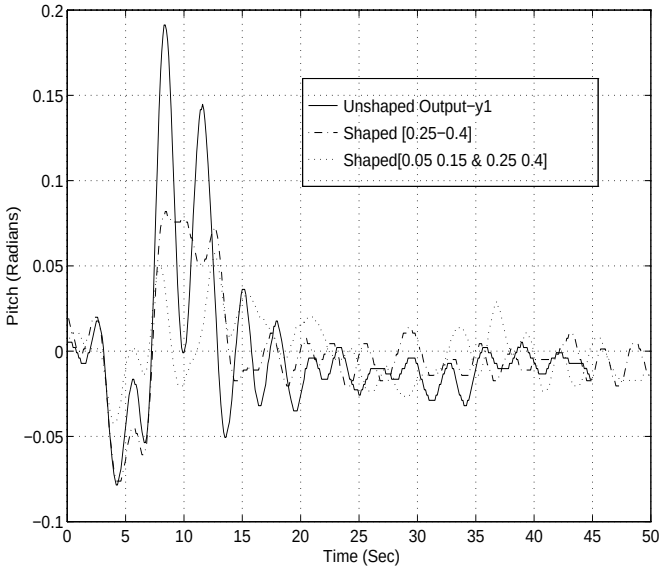

(a) Time domain.

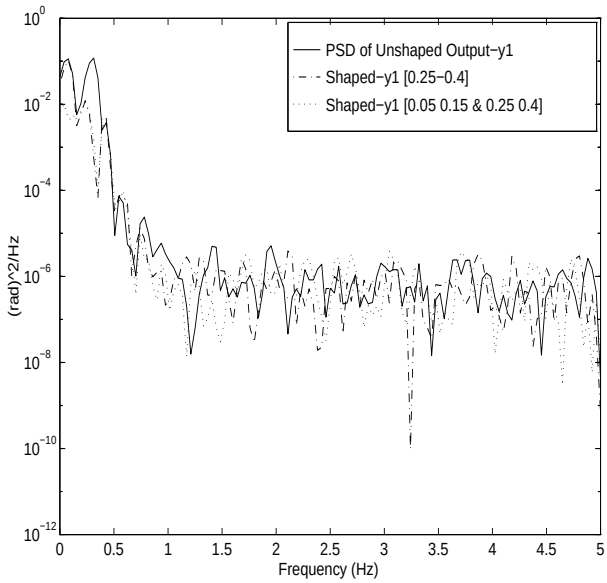

(b) Power spectral density.

Fig. 11 Pitch response with bandstop filtered doublet input, *u1* → *y1*.

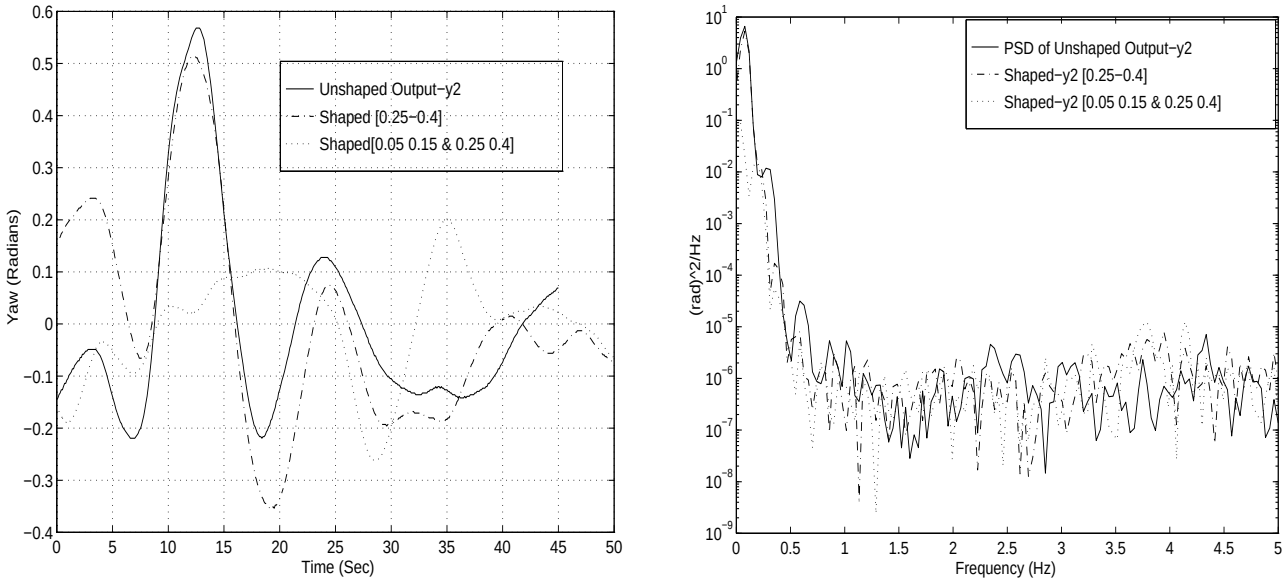

(a) Time domain. (b) Power spectral density.

Fig. 12 Yaw response with bandstop filtered doublet input, *u1* → *y2*.

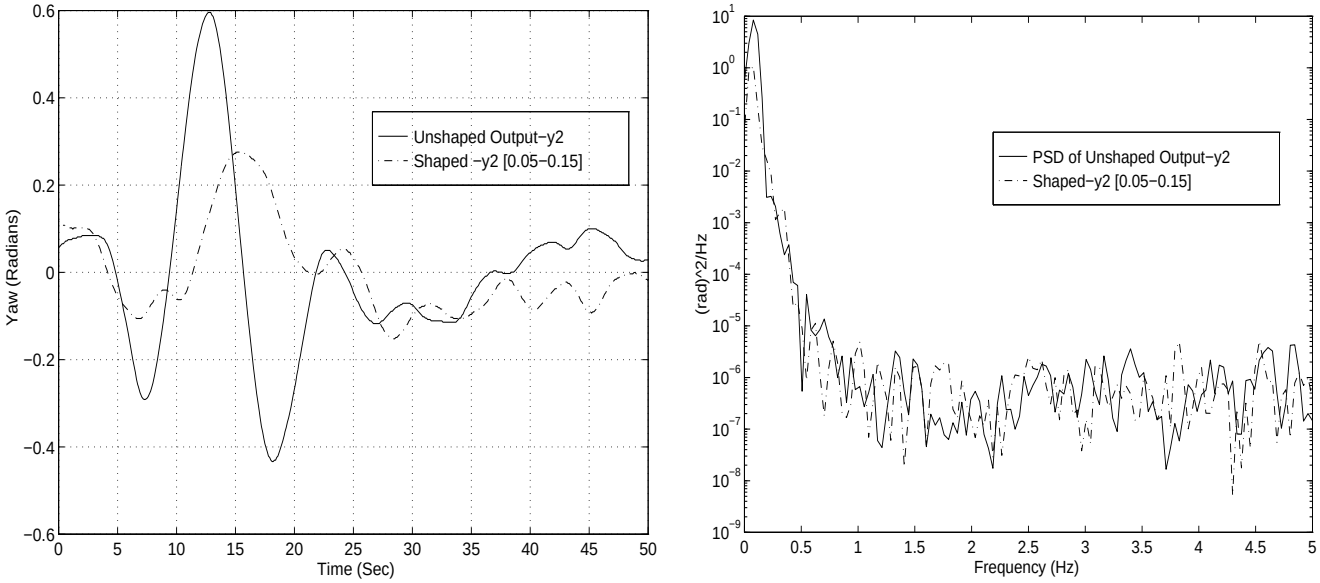

(a) Time domain. (b) Power spectral density.

Fig. 13 Yaw response with bandstop filtered doublet input, *u2* → *y2*.